The Journal of Neuroscience, August 1, 1998, *18*(15):5692–5705

Retinal Ganglion Cell Axon Progression from the Optic Chiasm to Initiate Optic Tract Development Requires Cell Autonomous Function of GAP-43

Kelly Kruger, Angie S. Tam, Cynthia Lu, and David W. Sretavan

Departments of Ophthalmology and Physiology, University of California, San Francisco, California 94143

Pathfinding mechanisms underlying retinal ganglion cell (RGC) axon growth from the optic chiasm into the optic tract are unknown. Previous work has shown that mouse embryos deficient in GAP-43 have an enlarged optic chiasm within which RGC axons were reportedly stalled. Here we have found that the enlarged chiasm of GAP-43 null mouse embryos appears subsequent to a failure of the earliest RGC axons to progress laterally through the chiasm–tract transition zone to form the optic tract. Previous work has shown that ventral diencephalon CD44/stage-specific embryonic antigen (SSEA) neurons provide guidance information for RGC axons during chiasm formation. Here we found that in the chiasm–tract transition zone, axons of CD44/SSEA neurons precede RGC axons into the lateral diencephalic wall and like RGC axons also express GAP-43. However unlike RGC axons, CD44/SSEA axon trajectories are unaffected in GAP-43 null embryos, indicating that GAP-43–dependent guidance at this site is RGC axon specific or occurs only at specific developmental times. To determine whether the phenotype results from loss of GAP-43 in RGCs or in diencephalon components such as CD44/SSEA axons, wild-type, heterozygous, or homozygous GAP-43 null donor retinal tissues were grafted onto host diencephalons of all three genotypes, and graft axon growth into the optic tract region was assessed. Results show that optic tract development requires cell autonomous GAP-43 function in RGC axons and not in cellular elements of the ventral diencephalon or transition zone.

Key words: retinal ganglion cell; axon pathfinding; optic tract; optic chiasm; GAP-43; growth cone; CD44; SSEA; mouse embryo development; diencephalon; hypothalamus

During development, embryonic RGC axons must find their way out of the retina into the optic nerve, grow through the optic chiasm, and extend along the optic tract to reach CNS targets. Recent studies have begun to identify the molecular basis of RGC axon guidance in a number of regions along this pathway. Within the retina, integrin and cadherin function seem to be involved in initial RGC axon outgrowth (Lilienbaum et al., 1995; Riehl et al., 1996), and chondroitin-sulfate proteoglycans and Ig superfamily axon guidance molecules have been proposed to direct RGC axons toward the optic disk (Brittis et al., 1992; Brittis and Silver, 1995) where netrin-1 acts locally to guide axons into the optic nerve (Deiner et al., 1997). At the opposite end of the pathway within target tissues such as the optic tectum of chick, the ephrin family of guidance molecules has been shown to influence retinal axon growth (Nakamoto et al., 1996; Frisen et al., 1998), and graded distributions of ephrins are proposed to establish the orientation of the retinotectal map (for review, see Orioli and Klein, 1997).

Attention has also focused on the optic chiasm and the optic tract, two other segments of the retinal pathway in which significant sorting and reordering of RGC axons take place. During development, RGC axons from the two eyes meet at the ventral diencephalon midline to form an X-shaped intersection known as the optic chiasm where RGC axons project specifically into either the contralateral or ipsilateral side of the brain. Although the molecular basis for chiasm pathfinding events remains to be elucidated, evidence points to a role for an early generated population of CD44- and stage-specific embryonic antigen (SSEA)-immunopositive neurons as well as radial glial cells in RGC axon guidance at the ventral diencephalon (Sretavan, 1993; Sretavan et al., 1994; Marcus and Mason, 1995; Mason and Sretavan, 1997). After forming the optic chiasm, RGC axons extend laterally and dorsally to establish the optic tract along the lateral wall of the diencephalon to reach visual targets in the thalamus and midbrain. In mammals where it has been best studied, the optic tract is not just an axon thoroughfare between the chiasm and visual targets. Different functional classes of RGC axons undergo substantial reordering in the tract to segregate into multiple overlapping retinotopic maps in advance of RGC axon arrival in the target regions (Reese and Cowey, 1988; Chan and Guillery, 1994). The molecular basis for this axon reordering is not understood. However, studies in amphibia have shown that RGC axon growth and pathfinding in more dorsal parts of the pathway as RGC axons approach the tectum appear to involve FGF and heparan sulfate (McFarlane et al., 1995; Walz et al., 1997). Despite the fact that proper development of anatomical pathways that route visual information in the adult brain requires RGC axons to accomplish pathfinding tasks successfully in both the optic chiasm and the optic tract, the mechanisms that enable RGC axons to progress from the chiasm to perform a different set of pathfinding tasks in the adjoining tract are not known.

Received Feb. 26, 1998; revised April 23, 1998; accepted May 13, 1998.

This research is supported by National Institutes of Health Grant EY10688, That Man May See Foundation, and EY02162 to the University of California, San Francisco, Department of Ophthalmology. D.W.S. is the recipient of a Jules and Doris Stein Professorship from Research to Prevent Blindness. We wish to thank Drs. Mark Fishman and Christophe Fankhauser for their gift of GAP-43 heterozygous mouse breeding pairs and Dr. Pate Skene for mouse mAb 91E12. We also thank Michael Deiner, Jessica Hanover, Chris Severin, and Fan Zhang for assistance in parts of this project.

Correspondence should be addressed to Dr. David Sretavan, Department of Ophthalmology, K107, University of California, San Francisco, 10 Kirkham Street, San Francisco, CA 94143.

Several anatomical observations suggest that RGC axons encounter a change in environment as they progress from the optic chiasm to establish the optic tract within the diencephalic wall. First, retinal axons entering the chiasm region are defasiculated and spread out from each other but once again become more tightly bundled as they grow laterally to form the optic tract (Reese et al., 1994; this paper). Second, ultrastructural analysis shows that embryonic day 16 (E16) mouse RGC axons leave their usual position just underneath the pial surface and extend within a deeper zone in the chiasm but again emerge closer to the pial surface as they approach the optic tract (Colello and Coleman, 1997). Although these documented changes in axon behavior during the transition from the chiasm into the tract are consistent with cellular and molecular differences between these two adjoining segments, other cellular elements actually serve as a bridge between these two regions. For example, CD44/SSEA neurons that reside in the ventral diencephalon (Sretavan et al., 1994; Marcus and Mason, 1995; Mason and Sretavan, 1997) project axons from the chiasm laterally and dorsally up to 1.5 mm into the lateral diencephalic wall (Sretavan et al., 1994) and anatomically bridge the transition zone. These neurons are present as an inverted V-shaped array of cells in the ventral diencephalon before the arrival of RGC axons, and their axons contribute to an early pathway in the lateral wall of the diencephalon, the tract of the postoptic commissure (Easter et al., 1993). Several lines of evidence implicate CD44/SSEA neurons in serving as a posteriorly located template involved in positioning the optic chiasm (Sretavan et al., 1994, 1995; Marcus and Mason, 1995; Wang et al., 1995). These neurons have also been proposed, in co-operation with radial glia, to provide ipsilateral and contralateral pathfinding cues (Wang et al., 1995). The spatial relationship between RGC axons and axons of CD44/SSEA neurons at the transition zone has not been precisely determined, and it is not clear whether these axons play any role in RGC axon progression from the optic chiasm into the lateral wall of the diencephalon to form the optic tract.

Here we have investigated the role of the intracellular protein GAP-43 in RGC axon guidance at the ventral diencephalon. GAP-43 is a highly abundant protein present in developing as well as in regenerating axons and growth cones (Skene, 1990; Benowitz and Routtenberg, 1997) that interacts with calmodulin (Alexander et al., 1988) and G-protein signaling pathways (Strittmatter et al., 1990). Although GAP-43 is expressed in certain glia cells (Deloulme et al., 1990; Curtis et al., 1992) where it may play as yet undefined functions, attention has been focused on the possible role of GAP-43 in axon growth. Transgenic mice overexpressing chicken GAP-43 postnatally in axons have an increased number of terminal sprouts at motor axon terminals and in hippocampal mossy fibers (Aigner et al., 1995), demonstrating the ability of GAP-43 to influence neuromuscular junction and axon terminal arbor development. Although function perturbation studies using antibodies (Shea, 1994; Shea and Benowitz, 1995) and antisense oligonucleotides (Aigner and Caroni, 1993) initially suggested a role in neurite extension, the findings in GAP-43 null mouse embryos of a grossly normal brain and long axonal projections (Strittmatter et al., 1995) indicated that GAP-43 is not essential for axon growth *in vivo*. A surprising result in GAP-43 null mice was the presence of an unusually enlarged optic chiasm during the period when RGC axons are actively growing through the ventral diencephalon. RGC axons in mutant mice were reported to "stall" at the chiasm and are delayed in their growth into the optic tract. Although these observations implicated GAP-43 function in RGC axon pathway formation, precisely how this protein influences RGC axon pathfinding is not known. Fundamental questions requiring investigation include the exact RGC axon pathfinding task at the ventral diencephalon requiring GAP-43, its specific requirement within RGC axons at the affected site in the retinal pathway, and whether the pathfinding defect can be functionally accounted for by loss of GAP-43 in RGC axons.

In this study we examined RGC axon pathfinding to the optic disk and the behavior of RGC axons growing into the ventral diencephalon of GAP-43 null embryos. The results show that initial RGC axon entry into the optic nerve and the ventral diencephalon and axon growth across the midline all occur apparently normally in the absence of GAP-43 function. In fact the first pathfinding defect is not seen until the earliest generated RGC axons attempt to leave the optic chiasm and grow dorsally into the diencephalic wall to form the optic tract, indicating that GAP-43 is involved in RGC growth cone interactions within the chiasm–tract transition zone. In this transition zone, GAP-43 may be specifically involved in RGC axon pathfinding because other axons expressing GAP-43 are not affected in their growth into the diencephalic wall. Lastly, although both ingrowing RGC axons and local axons resident in the transition zone express GAP-43, mix and match grafting of retinal tissues onto host ventral diencephalons demonstrates that failure of growth into the optic tract is best explained by the lack of GAP-43 function in RGC axons. Together these results identify the transition zone between the chiasm and tract as the first pathfinding site in the visual system where RGC growth cone interaction with the local environment is critically dependent on GAP-43.

MATERIALS AND METHODS

Animals. GAP-43 heterozygous mouse breeding pairs were obtained from Dr. Mark Fishman (Harvard University) (described in Strittmatter et al., 1995), and a breeding colony was established at the University of California, San Francisco. In all experiments, the day of vaginal plug detection was considered E0. Pregnant females were anesthetized using intraperitoneal injections of sodium pentobarbital, embryos were harvested, and the adult was killed using an overdose of sodium pentobarbital followed by bilateral thoracotomy. C57/Bl6 postnatal day 7 (P7) pups were anesthetized using hypothermia.

Genotyping. The genotype of all embryos used for experiments and of postnatal mice born in the breeding colony was determined by either DNA Southern blots or a PCR-based genotyping protocol obtained from Dr. Christophe Fankhauser (University of Zurich, Switzerland). For embryo genotyping, tail tissue, supplemented by limb tissue, was digested in 150 μl of buffer containing proteinase K (1 mg/ml) at 56°C for 30 min followed by boiling for 10 min. (In postnatal pups, ~3 mm of tail tissue was digested in 500 μl of proteinase K buffer overnight at 56°C.) Then 2.5 μl of buffer containing DNA was used as template in 100 μl PCR reactions in the presence of 2.5 mM $MgCl_2$. PCR primers used included GAP-43 forward primer (5′-GAGGCCGAGGCCAAGGAGAAGG-3′), GAP-43 reverse primer [5′-TCAGTGACAGCAGCAGGCACATCG-3′; product length, 314 base pairs (bp)], Neomycin forward primer (5′-ATGAACTGCAGGACGAGGCAGCG-3′), and Neomycin reverse primer (5′-CCATTCGCCGCCAAGCTCTTCA-3′; product length, 603 bp). PCR was performed on a Perkin-Elmer thermocycler 480 using a hot start procedure followed by 35 cycles of a two temperature protocol consisting of 72°C for 1 min and 95°C for 30 sec and a terminal extension step at 72°C for 10 min. DNA Southern blots were performed using a full-length rat GAP-43 cDNA as probe. Control experiments with Southern blots confirmed the reliability of the PCR protocol in identifying the genotype of embryos.

Retinal histology. Four percent paraformaldehyde (PFA)-fixed E13 and E16 retinas from wild-type and GAP43 homozygous null embryos were infiltrated overnight at 4°C with 30% sucrose in PFA; 12-μm-thick cryostat sections were cut, mounted on glass slides, and stained with the fluorescent nuclear dye 4,6-diamidino-2-phenylindole (DAPI) for 5 min

in 0.1 M PBS. After being rinsed in fresh PBS, sections were coverslipped and analyzed. Cell layer numbers and densities were obtained at midretina approximately halfway between the optic disk and the retinal periphery.

DiI labeling. DiI labeling of retinal ganglion cell axon projections in the retina and at the ventral diencephalon was performed using glass micropipettes to place small crystals of DiI (D282; Molecular Probes, Eugene, OR) into the retinas of embryos as described (Sretavan, 1990; Deiner et al., 1997). The axons of embryonic CD44/SSEA neurons were labeled by the placement of small DiI crystals in the ventral midline of the diencephalon as described (Sretavan et al., 1994).

Reconstruction of axon trajectories. During *in vivo* development, retinal axons grow through the optic chiasm following the curved surface of the brain to turn dorsally and grow into the initial portion of the optic tract. As a result, the trajectories of RGC axons cannot all be seen in a single flat optical plane. To reconstruct axon trajectories that extend from the ventral midline through the transition zone into the initial parts of the optic tract, we captured 30–60 images at 1–2 μm optical section thickness using a cooled CCD camera (photometrics PXL) and Deltavision Imaging software (Applied Precision, Issaquah, WA). Images of labeled axons in each optical section were then assembled using the "running projection" algorithm to identify and display the brightest pixel value at each pixel location within a stack of images. In some instances, montages of labeled axons were assembled manually using Adobe Photoshop. To present more clearly the overall organization of RGC axon trajectories from different genotype embryos at different ages, tracings were also made of stacked montages directly from the monitor screen and digitized.

To visualize the extent of CD44/SSEA axon growth along the lateral wall of the diencephalon in wild-type, heterozygous, and homozygous GAP-43 null embryos, we turned the brains from embryos that received DiI label in the retina onto their sides with the lateral surface of the diencephalon facing upward, and fluorescence images of DiI-labeled axons were acquired.

Immunolabeling. GAP-43 immunolocalization was performed using mouse mAb 91E12 (IgG1) ascites fluid (gift from Pate Skene, Duke University) at a concentration of 0.5 μg/ml. To reduce background labeling in mouse embryo tissues when using an anti-mouse IgG secondary antibody, we first preincubated sections with goat anti-mouse IgG (heavy + light) Fab fragments (15 μg/ml; Jackson ImmunoResearch, West Grove, PA.) in 0.1 M PBS with 0.05% Triton X-100 for 2 hr followed by additional blocking using 0.1 M PBS containing 10% normal donkey serum with 0.05% Triton X-100 for 30 min at room temperature (RT). Sections were then incubated with primary antibody for 18 hr at 4°C, washed with 0.1 M PBS four times for 5 min each, and incubated with goat anti-mouse IgG Cy3 antibody (1:400; Jackson ImmunoResearch) for 1–2 hr at RT. Sections were then washed in 0.1 M PBS four times for 5 min each and coverslipped using elvanol.

CD44 immunostaining was performed using rat mAb KM201 as previously described (Sretavan et al., 1994). Double immunolabeling of CD44 and GAP-43 was performed using rat mAb KM201 and mouse mAb 91E12 visualized by donkey anti-rat Cy3 and donkey anti-mouse Cy2, respectively. L1 immunostaining was performed using a rabbit polyclonal antibody (gift of C. Lagenaur; University of Pittsburgh) as described in Sretavan et al. (1994).

Immunoblots. Immunoblots were performed using mouse mAb 91E12. Retinas and ventral diencephalon tissues were harvested from E12 C57/Bl6 mouse embryos (Sretavan et al., 1994), and cortical tissue was obtained from P7 C57/Bl6 mouse pups. After dissection, tissues were placed directly in sample buffer (1% SDS, 5 mM EDTA, 10 mM DTT, 20% glycerol, bromophenol blue, and 10 mM Tris buffer, pH 7) and subjected to Dounce homogenization and boiling, after which samples were loaded onto 10% acrylamide gels. After electrophoresis, acrylamide gels were first fixed in 10% TCA, 10% acetic acid, and 20% isopropanol for 1 hr and rinsed in 25 mM Tris base, 192 mM glycine, and 1% SDS for 1 hr as described (Jacobson et al., 1986; Skene and Virag, 1989). Proteins were then electrophoretically transferred onto nitrocellulose paper at 4°C for 16 hr. Nitrocellulose blots were probed using mAb 91E12 (0.5 μg/ml) at 4°C for 16 hr, followed by alkaline phosphatase-conjugated secondary antibody at RT for 2 hr. All blockings and washes during immunoblotting were performed using 5% nonfat dry milk in 0.1 M PBS.

Retinal tissue grafting. E12.5 embryo litters resulting from the mating of GAP-43 heterozygous females with GAP-43 heterozygous males were used in grafting experiments. After tail tissue harvesting, retinas from individual embryos were dissected, maintained apart from retinas of other embryos, and labeled by incubation in DiI-containing cell culture medium (10 μl of DiI-saturated DMSO/EtOH [1:9] stock solution added to 2 ml of culture media [F12, N2 supplement (Life Technologies, Gaithersburg, MD), 100 U/ml penicillin, and 100 μg/ml streptomycin] that was filtered through a 5-μm-pore syringe filter to remove large DiI precipitates). After labeling for 30–45 min at 37°C in 5% CO_2, retinas from each embryo were then washed to remove free DiI by four sequential passages through 2 ml of fresh cell culture medium. Washed retinas from individual embryos were then stored separately in fresh cell culture medium at 37°C and 5% CO_2 (typically for 30–60 min) until grafted onto host diencephalon tissue preparations.

After removal of retinas, embryos were dissected to obtain ventral diencephalon preparations that included the optic nerves and chiasm and the ventral and lateral walls of the diencephalon, as well as the surrounding head tissue (for more detail, see Sretavan, 1993). The pia was then gently removed from the surface of the ventral diencephalon using fine jeweler's forceps, and diencephalon preparations were placed, ventral side up, on 8 μm pore-size transwells (Costar, Pleasanton, CA) containing culture media. The level of the medium was adjusted to just cover the surface of the diencephalon tissue.

Retina grafts were isolated from E12.5 DiI-labeled retinas cut up into approximately six small pieces using microscissors. Using a 10 μl pipettor, we transferred an individual retinal graft into a transwell containing a diencephalon preparation and gently placed the retinal ganglion cell side down onto the midline of the ventral diencephalon, in the region where RGC axons from the two eyes intersect to form the optic chiasm. Surface tension from the overlying media helped keep the grafts in place. Grafting was performed before obtaining genotype results. To obtain the various combinations of genotypes between host diencephalon and donor retinal grafts, we grafted the retina tissue from one embryo onto the diencephalon preparation of a second embryo, the retinal tissue from the second embryo onto the diencephalon preparation of a third embryo, and so on.

In control experiments, living retinal tissue grafts were substituted with either (1) retinal grafts that have been pre-fixed using 4% PFA for 30 min and rinsed four times in 2 ml volumes of culture media or (2) DiI-labeled pieces of adult liver tissue approximately the same size and shape as retinal grafts. In these control experiments, no DiI-labeled neurites were observed extending from either liver or PFA-fixed retinal grafts, demonstrating that there was no DiI transfer from the graft to the host diencephalon preparation. DiI-labeled axons were only seen emanating from grafts of living retinal tissues.

Reconstruction of axon trajectories in grafting experiments. After an incubation period of 40 hr at 37°C and 5% CO_2, the host diencephalon preparation with the attached retinal graft was fixed using 4% PFA. Preparations used for analysis were first selected for inclusion using the following criteria. (1) Preparations with no axon outgrowth were discarded, (2) grafts that moved from the original site of placement were discarded, and (3) preparations in which the region of the initial portion of the optic tract could not be visualized because of tissue overgrowth or shifting in culture were excluded. Based on these criteria, ~65–70% of grafts were analyzed.

To visualize and record the total extent of neurite outgrowth from retinal grafts on each diencephalon preparation, we turned preparations so that the transition zone 500 μm lateral to the midline was maximally in the center of focus, and multiple optical sections were recorded at different focal depths (as described above) to capture axons coursing from the midline to the transition zone as well as axons that grow past the transition zone into the lateral diencephalic wall. In each host diencephalon, the midline was located as a position equidistant from where the two optic nerves join the ventral diencephalon.

For quantitative measure of graft axon growth, the amount of labeled RGC axons in two adjacent regions of the host diencephalon straddling the transition zone 500 μm lateral to the midline was determined and compared (see Fig. 7*A*). The first region, a 100 × 200 μm area, corresponded to the region between 400 to 500 μm from the midline and consisted of axons approaching the transition zone that are in a position to cross the transition zone. The second region, also a 100 × 200 μm area, corresponded to the region between 500 to 600 μm from the midline and consisted of axons that have grown past the transition zone. In each region, DiI-labeled graft axons were traced, the tracings were digitized, and the amount of axon length was determined based on the number of black pixels using Adobe Photoshop histogram display. The amount of labeled graft axon in the second region was also expressed as a fraction of the amount of graft axon in the first region. A fraction close to 1

reflects a situation in which RGC axons have no apparent difficulty in growing through the transition zone, whereas a low fraction was obtained in cases in which RGC axons failed to progress for significant distances beyond the transition zone.

RESULTS

RGC axon guidance to the optic disk and growth into the optic nerve

Mouse embryos lacking GAP-43 have eyes indistinguishable in size and shape from eyes of wild-type littermates (Fig. 1*A*,*B*). No gross abnormalities in retinal development were observed in retinas of GAP-43 null embryos at E13 (data not shown) and E16 (Fig. *C*, *D*). Wild-type and homozygous null retinas contained approximately the same number of cell layers and were comparable in thickness and cell density.

Two pathfinding tasks newly generated RGC axons accomplish are to find their way within the retina from their site of origin toward the optic disk and then to exit through the disk to form the optic nerve. Sampling of the precision with which RGC axons in GAP-43 null embryos find their way toward the optic disk demonstrated that RGC axons in these embryos, like those in wild-type littermates, grew straight from their site of origin directly to the optic disk (Fig. 1*E*, *F*). This directed growth toward the disk, which is thought to involve in part the action of chondroitin sulfate and Ig superfamily molecules (Brittis et al., 1992; Brittis and Silver, 1995), thus apparently does not require GAP-43 function. After reaching the disk, RGC axons in GAP-43 null embryos all exited in an orderly manner and formed normal-sized optic nerves (Fig. 1*E*, *F*). This second pathfinding task that depends on local RGC axon interaction with optic disk netrin-1 via the axonal netrin-1 receptor DCC (deleted in colorectal cancer) (Deiner et al., 1997) was also not perturbed in the absence of GAP-43.

Axon ingrowth into the ventral diencephalon is unaffected in GAP-43 null embryos

In normal development, RGC axons have arrived at the ventral diencephalon by E12.5 and have begun to cross the midline to initiate the formation of the optic chiasm (Colello and Guillery, 1990; Godement et al., 1990; Sretavan, 1990). The approximate numbers of RGC axons entering the ventral diencephalon, their axon trajectories, and the extent of growth toward the ventral midline were compared between E12.5 wild-type, heterozygous, and homozygous GAP-43 null embryos after DiI labeling at the optic disk. Observations in DiI-labeled whole-mount preparations of the ventral diencephalon (Fig. 2*A*,*D*) and reconstructions of axon trajectories (Fig. 2*B*,*C*,*E*,*F*) indicated approximately equal numbers of RGC axons enter the ventral diencephalon in wild-type (Fig. 2*A–C*), heterozygous (data not shown), and GAP-43 null (Fig. 2*D–F*) embryos. A prominent feature of RGC axon ingrowth at the ventral diencephalon is the noticeable change in trajectory as axons approach the midline (Sretavan et al., 1994; Marcus and Mason, 1995). In wild-type embryos, RGC axons after entering the ventral diencephalon change from a posteriorly directed course to run perpendicular or in a slightly anterior direction toward the midline (Fig. 2*A–C*; *dotted arrow* in *A*). This characteristic change in RGC axon trajectory was also observed in GAP-43 null embryos (Fig. 2*D–F*; *dotted arrow* in *D*), indicating that RGC axons in GAP-43 null embryos respond to cues governing early RGC axon ingrowth. Lastly, wild-type E12.5 embryos within a given litter often vary in the extent of RGC ingrowth at the midline (compare Fig. 2*B* with *C*). The same degree of variation was also observed between E12.5 GAP-43 null

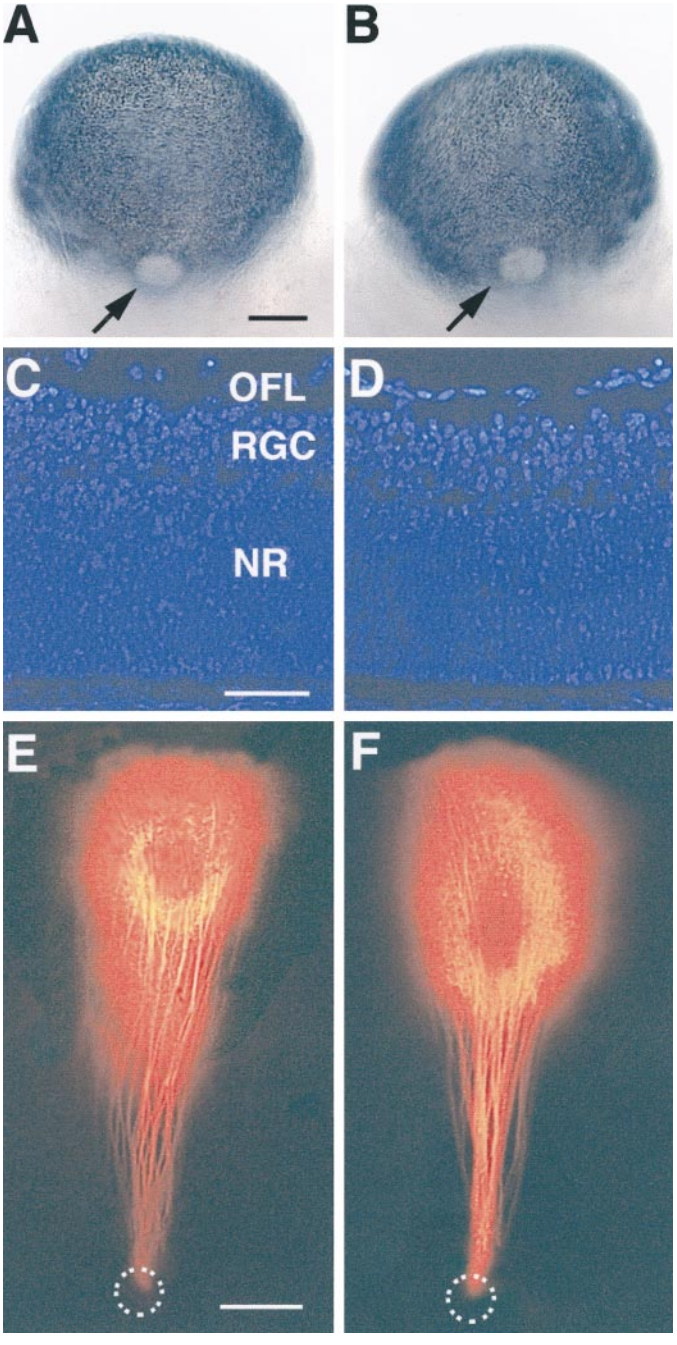

Figure 1. Eye morphology, retinal cytoarchitecture, and RGC axon pathfinding to the optic disk in wild-type and GAP-43 homozygous null embryos. *A*, *B*, Posterior views of the eye in an E16 wild-type (*A*) and a GAP-43 homozygous null embryo (*B*). *Arrows* indicate the optic disk. The overall size and shape of the eye, the pigmentation pattern, and the size of the optic disk were comparable in wild-type and homozygous null embryos. Scale bar, 250 μm. *C*, *D*, DAPI-stained retinal sections from a E16 wild-type (*C*) and a littermate GAP-43 homozygous null embryo (*D*). Retinal thickness, number of cell layers, and cell density were very similar in all embryos. *OFL*, Optic fiber layer; *RGC*, retinal ganglion cell layer; *NR*, neural retina. See text for details. Scale bar, 50 μm. *E*, *F*, RGC axon trajectories toward the optic disk following DiI spot labeling in the retina of a wild-type (*E*) and a littermate GAP-43 homozygous null embryo (*F*). RGC axons in embryos of both genotypes grow in straight trajectories from their sites of origin to the optic disk (*dotted circles*) where they exit and grow into the optic nerve. Scale bar, 100 μm.

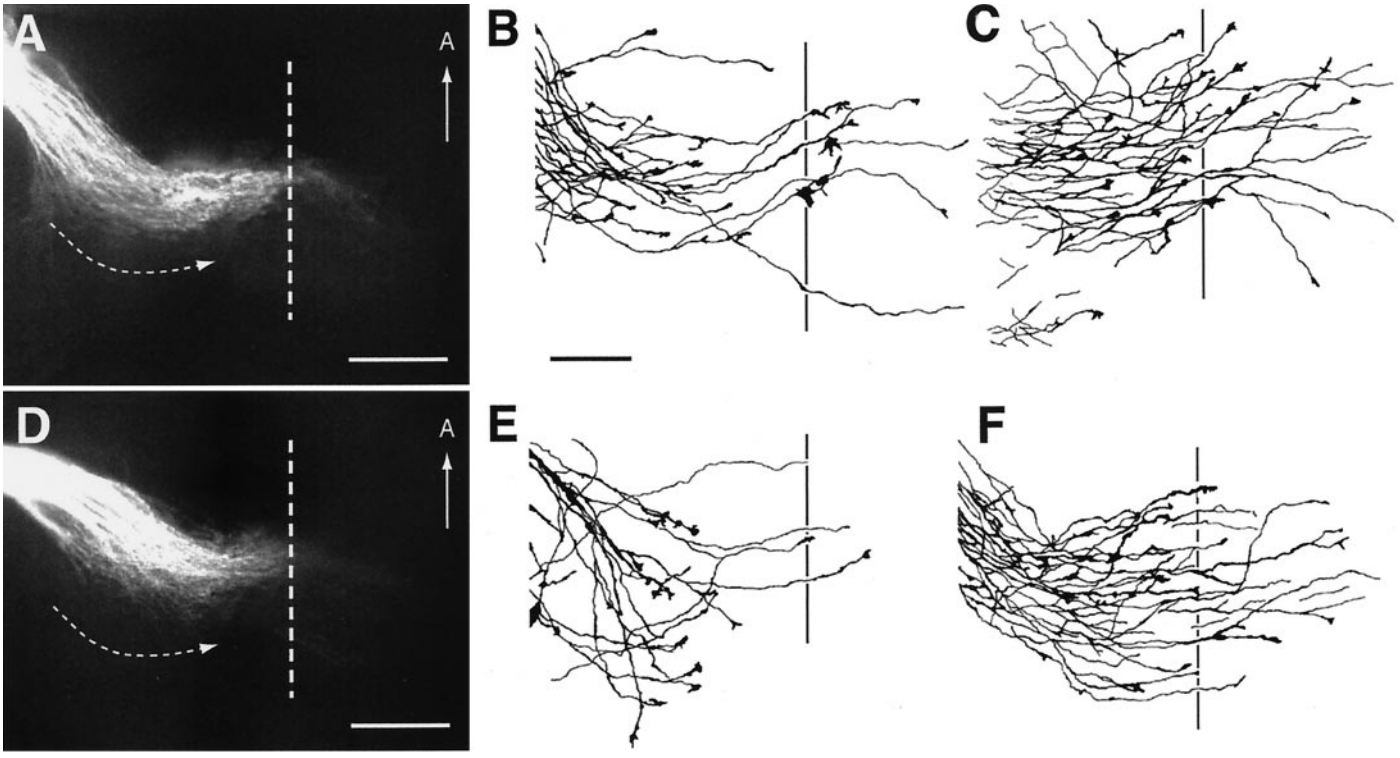

Figure 2. RGC axon growth into the ventral diencephalon of E12.5 wild-type and GAP-43 homozygous null embryos. All *panels* show the ventral view of the diencephalon. Anterior (*A*) is *up*. The *vertical solid* and *dashed lines* represent the midline. *Panel A*, RGC axon ingrowth into the ventral diencephalon of an E12.5 wild-type embryo visualized by labeling the RGC axon projection from one eye with DiI. At this age, RGC axons have entered the ventral diencephalon, and some axons have crossed the midline, but an optic tract is not yet evident. The *dotted line* with *arrowhead* illustrates the characteristic change in axon trajectory as RGC axons enter the ventral diencephalon in a posterior-medial direction and then turn to grow perpendicular or in a slightly anterior direction toward the midline. Scale bar, 200 μm. *Panels B*, *C*, RGC axon trajectories from two other E12.5 wild-type littermate embryos. These two figures also illustrate the variation in RGC axon ingrowth that can be seen at this age within a given litter. Scale bar, 100 μm. *Panel D*, RGC axon growth into the ventral diencephalon of an E12.5 GAP-43 homozygous null embryo visualized by labeling the RGC axon projection from one eye with DiI. RGC axons in GAP-43 null embryos, like their counterparts in wild-type embryos (*panel A*), exhibit the same characteristic change in trajectory after entering the ventral diencephalon (*dotted line* with *arrowhead*). The extent of axon ingrowth is indistinguishable from that of wild-type embryos (*panel A*). Scale bar, 200 μm. *Panels E*, *F*, RGC axon trajectories from two E12.5 littermate GAP-43 homozygous null embryos. The trajectories and extent of RGC axon ingrowth are like those seen in E12.5 wild-type embryos (*panels B*,*C*). RGC axons in GAP-43 null embryos have no apparent difficulty entering the ventral diencephalon or crossing the midline. Scale bar, 100 μm.

embryos of the same litter (compare Fig. 2*E* with *F*). Thus, the overall pattern and extent of RGC axon ingrowth into the ventral diencephalon at E12.5 were indistinguishable in wild-type and GAP-43 null embryos.

The findings that embryonic retinal development is normal and that RGC axons arrive on time at the E12–12.5 ventral diencephalon in GAP-43 null embryos compared with wild-type embryos indicate that GAP-43 seems not to be required for the differentiation of RGCs. In addition, although GAP-43 is expressed in embryonic RGC axons within the optic fiber layer in the retina and in axons coursing in the optic nerve (see Fig. 5*F*), it is apparently not essential for RGC axon growth within these early segments of the retinal pathway.

RGC axons cross the midline but fail to grow into the optic tract

By E14, RGC axons in wild-type embryos have grown beyond the ventral midline and established the optic tract within the diencephalic wall (Fig. 3*A*). Similar to that in wild-type embryos, RGC axons in E14 GAP-43 null embryos have also grown across the midline. In contrast, however, RGC axons in GAP-43 null embryos do not extend into the diencephalic wall to form an optic tract. Instead, they appear to stop at a distance of ~450–500 μm lateral to the midline (Fig. 3*B*), a position that we designate as the chiasm–tract transition zone. Often, some RGC axons form an ectopic projection that runs anteriorly within the diencephalon (Fig. 3*B*, *arrow*); such ectopic projections have not been observed in wild-type embryos. The failure of axon growth at the chiasm–tract transition zone was a penetrant phenotype. Although a few axons can occasionally be seen in some homozygous null animals to grow into the tract, the vast majority of RGC axons failed to progress through the chiasm–tract transition zone in every homozygous null embryo identified at E14–E16 ($n = 17$). RGC axons in heterozygous embryos are not affected in their growth through the chiasm–tract transition zone. In heterozygous embryos at this and subsequent ages, no differences in the development of RGC axon projections were observed compared with wild-type embryos.

It is worth noting that in wild-type animals, in addition to the main bundle of RGC axons forming the optic chiasm (Fig. 3*A*, *asterisk*), some RGC axons travel in a more posterior region (Fig. 3*A*, *arrowheads*) following the same general course as the main RGC axon bundle. These RGC axons are intermixed with CD44/SSEA neurons and their axons that are found posterior to the main bundle of the optic chiasm (Sretavan et al., 1994; Marcus and Mason, 1995). This population of more posteriorly located RGC axons is also found in GAP-43 null embryos (Fig. 3*B*,

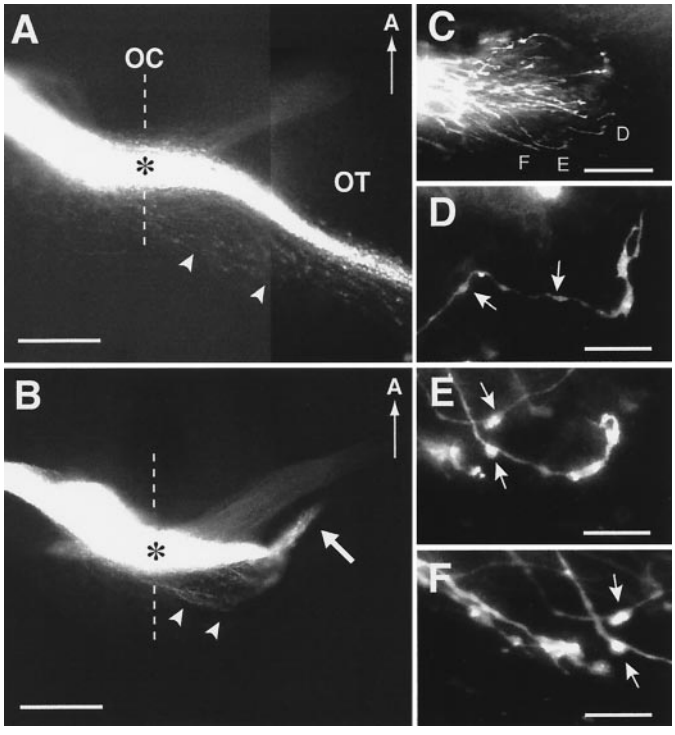

Figure 3. RGC axon projection patterns in wild-type and GAP-43 homozygous null embryos at E14 and examples of growth cones in GAP-43 homozygous null embryos. *Panel A*, RGC axon projections in the optic chiasm (*OC*) and optic tract (*OT*) regions of an E14 GAP-43 wild-type embryo visualized by labeling the RGC axon projection from one eye with DiI. At this age, a substantial number of RGC axons have grown through the optic chiasm into the optic tract that extends dorsally along the lateral wall of the diencephalon. Note the presence of RGC axons (*arrowheads*) that run posteriorly from the main bundle of RGC axons (*) forming the optic chiasm and the optic tract. The midline is indicated by the *dotted line*. Scale bar, 400 μm. *Panel B*, RGC axon projections in an E14 GAP-43 homozygous null embryo. In contrast to RGC axons in wild-type embryos at this age, RGC axons in GAP-43 null embryos do not project into the lateral diencephalic wall to initiate formation of the optic tract. Instead, after crossing the midline, they extend for ~450 μm away from the midline to reach the transition zone between the chiasm and the optic tract but then turn away. Often some axons form an ectopic bundle (*white arrow*) and project in an anterior direction. Note that both RGC axons in the main bundle (*) as well as RGC axons in the posterior region (*arrowheads*) fail to progress from the optic chiasm into the lateral diencephalic wall. Scale bar, 400 μm. *Panel C*, DiI-labeled RGC axons in the chiasm–tract transition zone region in an E14 GAP-43 homozygous null embryo. The axons labeled *D–F* are shown in higher magnification in *panels D–F*, respectively. Scale bar, 100 μm. *Panels D–F*, RGC axons and growth cones in the GAP-43 homozygous null embryo shown in *panel C*. Compared with RGC axons in C57/Bl6 embryos (Bovolenta and Mason, 1987; Sretavan, 1993; Godement et al., 1994) and GAP-43 wild-type embryos (data not shown) of the same age in this region, GAP-43 null axons often have multiple swellings along their axon trunks (*arrows*) and unusually elongated growth cones up to 25 μm in length. Scale bar, 25 μm.

arrowheads) and, like RGC axons in the main bundle (Fig. 3*B*, *asterisk*), also does not progress beyond a distance of 450–500 μm lateral from the midline to grow into the optic tract. Thus, the absence of GAP-43 function during development seems to interfere with the progression of all RGC axons through the chiasm–tract transition zone and affects initial formation of the optic tract.

Analysis of RGC axons approaching the transition zone region in GAP-43 null embryos revealed axons and growth cones with abnormal morphologies (Fig. 3*C–F*). In wild-type embryos, RGC axons at this site, as in other parts of the retinal pathway, have a relatively smooth axon trunk ending in a growth cone ~10–15 μm in length (Bovolenta and Mason, 1987; Sretavan and Reichardt, 1993; Godement et al., 1994; Mason and Wang, 1997). In contrast, RGC axons in GAP-43 null embryos turn away from the optic tract region, and their axons are characterized by many swellings distributed along axon trunks (Fig. 3*D–F*, *arrows*) that terminate in abnormally long growth cones extending up to 25 μm in length (Fig. 3*D*,*E*).

Histological examination of the optic chiasm–optic tract transition zone in E13 and E14 GAP-43 null embryos revealed no gross cytoarchitectural differences in this brain region compared with wild-type embryos. Overall cell density and thickness of the ventricular zones and mantle layer were indistinguishable between wild-type and GAP-43 null embryos. Thus the RGC axon guidance defect at the transition zone does not seem to be secondarily attributable to any detectable cell differentiation or migration defect in this region of the diencephalon.

Appearance of disorganized RGC axon trajectories within the optic chiasm

In older embryos at E16, after more RGC axons have grown into the region of the optic chiasm, disorderly axon trajectories become readily apparent within the optic chiasm itself. In wild-type animals at E16, RGC axons grow along fairly straight trajectories to cross the midline (Fig. 4*A–C*). In contrast, in GAP-43 null embryos, the retinal projection pattern is characterized not only by an absent optic tract but also by an enlarged optic chiasm (Fig. 4*D*) (see also Strittmatter et al., 1995). This enlarged optic chiasm is composed of disorganized RGC axons (Fig. 4*E*,*F*), many of which have grown in abnormal trajectories within the chiasm, including axons that appear to head back across the midline (Fig. 4*E*, *arrowheads*). Thus, between E14 and E16, the pathfinding defect originally localized to a region 500 μm lateral to the midline spreads in a retrograde manner resulting in abnormal axon trajectories within the chiasm proper. Abnormal trajectories were seen in all regions of the chiasm before and after axons have crossed the midline.

Although other explanations are possible, one reason for this apparent retrograde spread of phenotype may simply be the fact that large numbers of RGC axons that enter the optic chiasm at later stages of development back up against the initial pathfinding defect at the optic chiasm–optic tract transition zone. Subsequently, disorganized trajectories develop resulting in an overall enlarged retinal projection at the chiasm region. The finding that the initial pathfinding defect occurs 450–500 μm lateral to the midline indicates that an analysis of how GAP-43 is involved in visual system pathfinding should focus on E13 and E14 RGC axons at the chiasm–tract transition zone.

Intermixing of RGC axons and CD44/SSEA axons at the chiasm–tract transition zone

The cellular interactions mediating RGC axon guidance at the optic chiasm–optic tract transition zone are not well characterized. Previous work examining the cellular environment of the ventral diencephalon region revealed a close association between early RGC axons and a population of CD44- and SSEA-immunopositive neurons (Sretavan et al., 1994; Marcus and Mason, 1995). Before the arrival of RGC axons, the cell bodies of these CD44/SSEA neurons are arrayed as an inverted V shape with the tip of the V pointing anteriorly at the midline. Incoming RGC axons appear to form the posterior boundary of the optic chiasm along the anterior edge of the array of CD44/SSEA

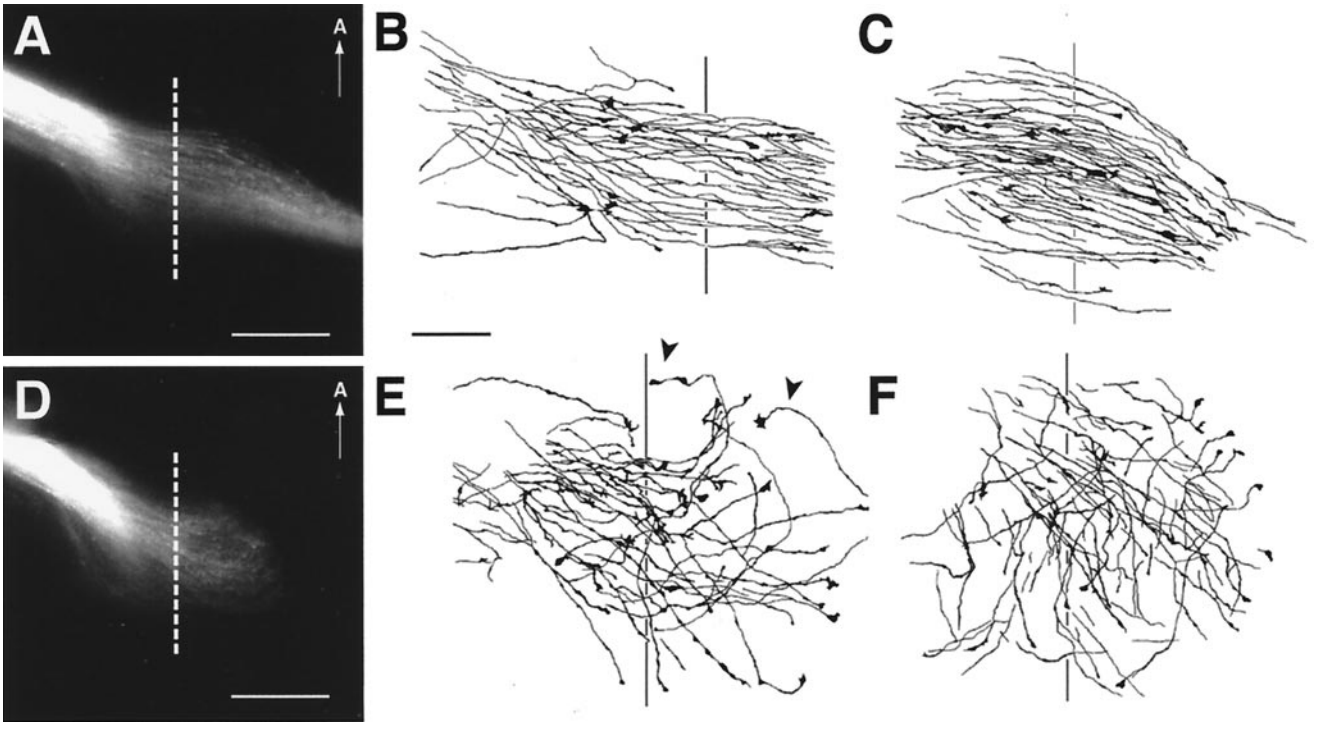

Figure 4. Patterns of RGC axon ingrowth in wild-type and GAP-43 homozygous null embryos at E16. *A*, RGC axons at the optic chiasm of an E16 GAP-43 wild-type embryo. The overall pattern of RGC axon ingrowth is similar to that seen at E14 but with additional axons added to the pathway. The *vertical dotted line* represents the midline. Scale bar, 400 μm. *B*, *C*, RGC axon trajectories in two E16 GAP-43 wild-type littermate embryos. Individual RGC axons traverse the optic chiasm in relatively straight trajectories. The *vertical line* represents the midline. Scale bar, 100 μm. *D*, RGC axon projections in an E16 GAP-43 homozygous null embryo. There is no optic tract, and RGC axons have formed a rounded enlarged optic chiasm. The *vertical dotted line* represents the midline. Scale bar, 100 μm. *E*, *F*, RGC axon trajectories from two E16 GAP-43 homozygous null littermate embryos. RGC axon trajectories in these animals are disorganized, and axons do not run in a parallel manner to cross the midline. In fact, some growth cones are seen heading in directions opposite to the normal course (*arrowheads* in *E*) and likely belong to axons that have turned away from the initial portion of the optic tract to grow in abnormal trajectories within the chiasm. Scale bar, 100 μm.

neurons (Sretavan et al., 1994; Marcus and Mason, 1995), and evidence supports a role for these neurons in RGC axon guidance (Sretavan et al., 1995; Wang et al., 1995). Of note, CD44/SSEA neurons send long axons laterally and dorsally up to 1.5 mm in length into the diencephalic wall (Sretavan et al., 1994) (see also schematics in Fig. 5*A*,*B*). Given the relationship between CD44/SSEA neurons and RGC axons in the ventral diencephalon, it seemed likely that these two axon populations might also be closely associated laterally at the transition zone.

To examine the relationship between RGC axons and axons of CD44/SSEA neurons at the transition zone in E13–E13.5 embryos, RGC axons were first labeled with DiI placed into the retina of fixed embryos. Horizontal tissue sections were then obtained from such DiI-labeled embryos through the transition zone, and RGC and CD44/SSEA axons were labeled with antibodies against L1, a cell surface molecule present on both axonal populations (Sretavan et al., 1994). Results from these double-label experiments show that in the transition zone, most RGC axons (Fig. 5*C*, *yellow orange*) run anterior to the axons of the CD44/SSEA neurons (Fig. 5*C*, *green*). However, a substantial number of RGC axons course in a more posterior region (Fig. 5*C*, *arrow*) and are intermixed with axons of the CD44/SSEA neurons. This spatially overlapping relationship between a subpopulation of RGC axons and CD44/SSEA axons is maintained more dorsally within the initial parts of the optic tract (Fig. 5*D*). Because CD44/SSEA axons have been shown to project into the lateral diencephalic wall by E11 (Sretavan et al., 1994), whereas RGC axons do not begin to enter the optic tract until E13 (Colello and Guillery, 1990; Godement et al., 1990; Sretavan, 1990), there is a 2 d interval between the growth of CD44/SSEA axons and the subsequent growth of a subpopulation of RGC axons through the transition zone region.

Expression of GAP-43 in the transition zone

As a first step to investigate how the lack of GAP-43 may lead to a defect in RGC pathfinding, the spatial pattern of GAP-43 expression was examined in the embryonic mouse visual system using anti-GAP-43 antibody (mAb 91E12). Protein immunoblots of P7 mouse cortex tissue homogenate demonstrated an immunoreactive band of ~45 kDa (Fig. 5*E*, *lane 1*), consistent with the known molecular weight of GAP-43 present in postnatal rat cortex (Jacobson et al., 1986). Immunoreactive bands of a similar size were also found in homogenates obtained from E12 mouse retina (Fig. 5*E*, *lane 2*) and E12 ventral diencephalon (*lane 3*). At E12, RGC axons have exited the eye into the optic nerve but have yet to arrive at the ventral diencephalon. The presence of a GAP-43–immunoreactive band in the retina is consistent with the expression of GAP-43 in RGC axons. However the finding of an immunoreactive band in the ventral diencephalon was unexpected and indicated the presence of other cells expressing GAP-43.

Immunostaining of E12 retinal tissue sections revealed GAP-43 immunoreactivity in the optic fiber layer and in the optic disk region leading into the optic nerve consistent with the

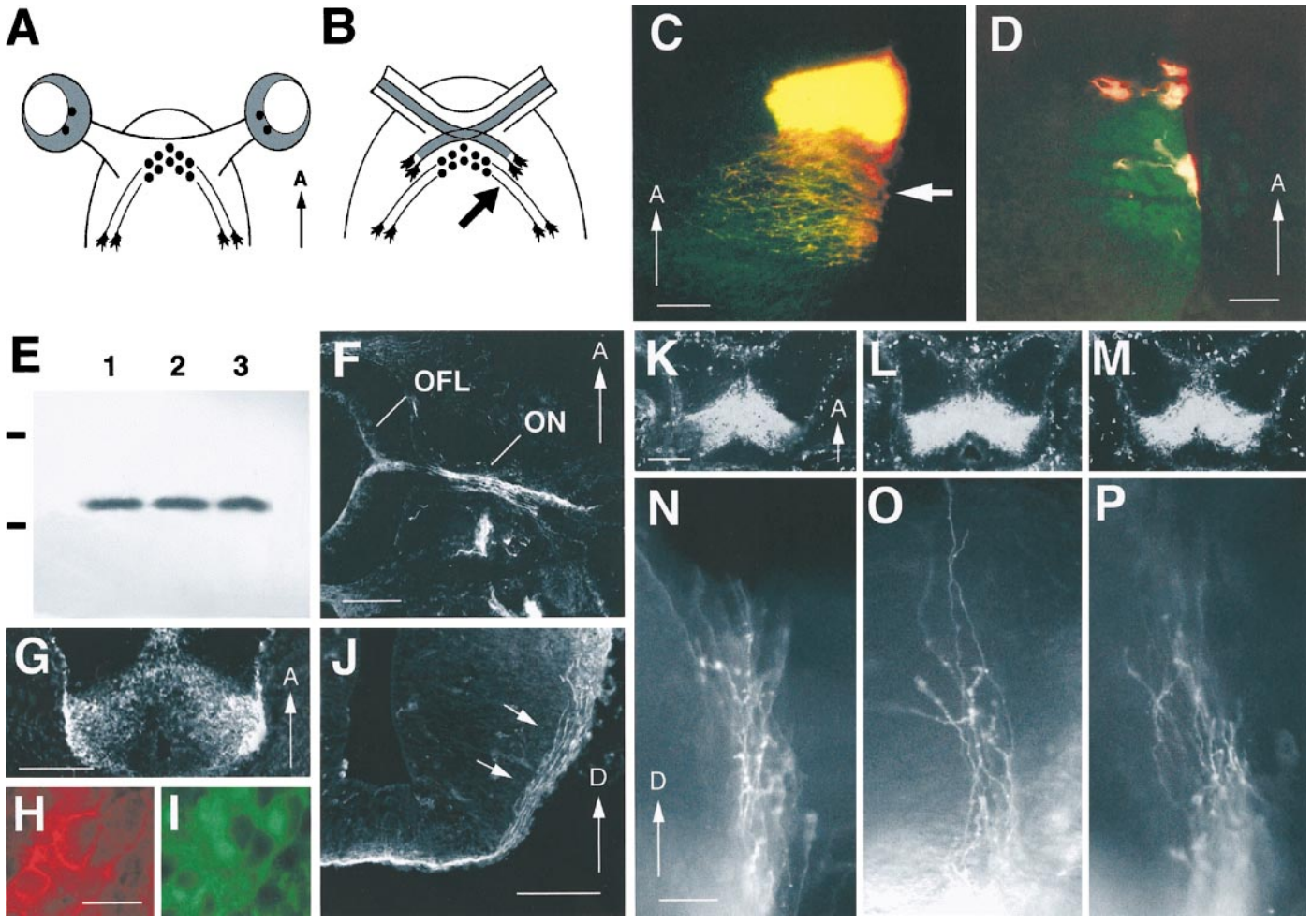

Figure 5. Expression of GAP-43 protein in RGC axons and CD44/SSEA neurons and development of CD44/SSEA neurons and their axons in GAP-43 null mutant embryos. *A*, *B*, Schematic diagrams showing the relationship between CD44/SSEA neurons and their axons with RGC axons at the ventral diencephalon. *A*, At E11, before the arrival of RGC axons at the ventral diencephalon, CD44/SSEA neurons (*small filled circles*) are present approximately in the future region of the optic chiasm (*shaded regions* represent the retinas). *B*, At E12.5–E13, RGC axons have grown into the ventral diencephalon and begun to establish the X-shaped optic chiasm in close relationship with the CD44/SSEA neurons and their axons. The *arrow* points to the region located ~450 μm lateral to the midline that we have identified as the chiasm–tract transition zone. (The retinas have been omitted in *B*.) *C*, Double-exposure photograph showing, in the horizontal plane of section, the relationship between RGC axons and the axons of CD44/SSEA neurons at the optic chiasm–optic tract transition zone in an E13.5 C57/Bl6 embryo. In this experiment, RGC axons were first labeled with DiI, and then both RGC axons and axons of CD44/SSEA neurons were labeled with an anti-L1 antibody and visualized using FITC (*green*). RGC axons that are doubly labeled with DiI (*red*) and FITC (*green*) appear *yellow-orange* in this photo. Axons of CD44/SSEA neurons, which express L1, appear *green*. Note the mixing of a subpopulation of RGC axons in the area occupied by axons of CD44/SSEA neurons (*white arrow*). Because of the curvature of the diencephalon, labeled axons outside of the transition zone are not present in this section. Scale bar, 100 μm. *D*, Double-exposure photograph from the experiment in *C* showing a more dorsal level ~1 mm from the ventral midline at a higher magnification. At this location, the partially overlapping distribution of RGC axons and CD44/SSEA axons is maintained. In this photo, three RGC growth cones are cut in cross-section. Two growth cones are found anterior to the L1-labeled CD44/SSEA axons, but one is found within the region occupied by CD44/SSEA axons (*green*). Scale bar, 25 μm. *E*, Immunoblot using anti-GAP-43 mAb 91E12 demonstrating the presence of a single immunoreactive band of ~45 kDa from P7 mouse cortex (*lane 1*), E12 wild-type mouse retina (*lane 2*), and E12 wild-type mouse ventral diencephalon (*lane 3*). *Black horizontal bars* (*left*) represent molecular weight markers; *top*, 68 kDa; *bottom*, 43 kDa. *F*, Horizontal section through the eye and optic nerve of an E12 wild-type embryo. GAP-43 immunoreactivity is present in the optic fiber layer (*OFL*), at the optic disk, and in the optic nerve (*ON*), consistent with the presence of this protein in RGC axons. Scale bar, 100 μm. *G*, Horizontal section through the ventral diencephalon of an E12 wild-type embryo. GAP-43 immunoreactivity is present in cells distributed as an inverted V-shaped array in the ventral diencephalon, corresponding to the inverted V-shaped array of CD44/SSEA neurons reported in previous studies. Scale bar, 100 μm. *H*, *I*, E12 ventral diencephalon cells that express CD44 (*H*) and are also immunoreactive for CD44 (*I*). Scale bar, 10 μm. *J*, Coronal section through the diencephalon of an E12 wild-type embryo. GAP-43 immunoreactivity is present within the axons of the CD44/SSEA neurons (*arrows*) that run along the lateral wall of the diencephalon. Scale bar, 100 μm. *K–M*, Horizontal cryostat sections demonstrating the presence of anti-CD44 immunoreactivity on CD44/SSEA neurons in the ventral diencephalon in E12 wild-type (*K*), heterozygous (*L*) and GAP-43 homozygous null (*M*) embryos. The absence of GAP-43 during development does not grossly affect the position of these neurons and expression of CD44. Scale bar, 100 μm. *N–P*, Lateral view of the diencephalic wall showing DiI-labeled axons of CD44/SSEA neurons projecting dorsally in E12 wild-type (*N*), heterozygous (*O*), and homozygous GAP-43 null (*P*) embryos. Only the dorsal one-half of the CD44/SSEA axon projection is shown in each *panel*. The distal-most extent of labeled axons is found ~1 mm from the ventral midline. Scale bar, 100 μm.

presence of this protein in E12 RGC axons (Fig. 5*F*). In E12 tissue sections of the ventral diencephalon, GAP-43 was found in a group of cells arrayed in an inverted V-shaped pattern (Fig. 5*G*), identical to the inverted V-shaped array of CD44/SSEA neurons (Sretavan et al., 1994). The coexistence of CD44 and GAP-43 in the same neurons was confirmed in double-immunolabeling experiments (Fig. 5*H*,*I*). GAP-43 expression was not restricted to the cell bodies of CD44/SSEA neurons but was also present in their axons (Fig. 5*J*, *arrows*) that by E12 have progressed dorsally beyond the transition zone into the diencephalic wall.

Growth of CD44/SSEA axons is unaffected in GAP-43 null embryos

The presence of GAP-43 in both RGC axons and axons of CD44/SSEA neurons and the fact that both grow through the transition zone into the lateral wall of the diencephalon suggested the possibility that GAP-43 is generally required in axons to grow through the chiasm–tract transition zone and that the development of CD44/SSEA neurons and their axonal growth might also be affected in GAP-43 null embryos. The absence of GAP-43 during development does not appear to lead to gross abnormalities in the numbers or distribution of CD44/SSEA neurons at the ventral diencephalon. Approximately equivalent anti-CD44 immunoreactivity was detected in CD44/SSEA neurons in wild-type, heterozygous, and homozygous animals (Fig. 5*K–M*). To examine the growth of CD44/SSEA axons along the lateral diencephalic wall, we applied DiI crystals to the ventral midline to label anterogradely CD44/SSEA axons from their cell bodies. Results showed that CD44/SSEA axons were present in wild-type, heterozygous, and homozygous animals and moreover projected in approximately the same dorsal orientation for equivalent distances along the lateral diencephalic wall (Fig. 5*N–P*). These results indicated that not all axonal populations require GAP-43 to progress from the ventral midline region into the lateral wall of the diencephalon and suggest that intrinsic differences may exist between RGC and CD44/SSEA axons in their interactions with the transition zone environment. An alternative is that the transition zone environment itself changes in the 2 d interval between the ingrowth of CD44/SSEA and RGC axons.

Retinal tissue grafting to assess the site of loss of function

The finding that CD44/SSEA neurons and axons express GAP-43 raised the additional question of whether the RGC axon pathfinding defect at the transition zone was caused by the lack of GAP-43 function in RGC growth cones or whether the absence of GAP-43 in CD44/SSEA neurons and axons may have somehow contributed to the defect. The earliest RGC axons arriving at the ventral diencephalon mix into and grow along the anterior part of the CD44 neuron array, followed subsequently by the accumulation of later-arriving RGC axons anteriorly to form the main bundle of the optic chiasm (Sretavan et al., 1994). The manner in which the optic chiasm is built up anteriorly after initially intermixing with CD44/SSEA neurons has led to the proposal that these neurons resident in the ventral diencephalon serve as a posterior template for positioning of the optic chiasm (Sretavan et al., 1994), a possibility receiving some support by findings *in vitro* (Sretavan et al., 1994; Wang et al., 1995) and *in vivo* (Sretavan et al., 1995). The fact that the earliest RGC axons entering the initial part of the optic tract are intermixed with axons of CD44/SSEA neurons (Fig. 5*D*) and that later-generated RGC axons then form the main bundle at the transition zone anterior to CD44/SSEA axons (Fig. 5*C*) suggested a parallel relationship to that occurring during optic chiasm formation. The apparently normal CD44/SSEA axon trajectories (Fig. 5*N–P*) eliminated a simple model in which the lack of GAP-43 in CD44/SSEA axons resulted in abnormal axon growth into the lateral diencephalic wall and secondarily led to guidance defects in RGC axons that follow. However, it remained possible that CD44/SSEA neurons in GAP-43 null embryos were perturbed in a more subtle manner that affected RGC axon pathfinding.

To determine whether GAP-43 acts cell autonomously within RGC growth cones or in cellular components of the pathway, a set of mix-and-match grafting experiments was performed in which retinal tissue of a given embryo (from a GAP-43 heterozygous female mated to a heterozygous male) was grafted onto the host ventral diencephalon of a second embryo of the same litter, resulting in different combinations of wild-type, heterozygous, and homozygous retinal tissue grafted onto host diencephalons of all three genotypes (Fig. 6*A*). (The genotypes of embryos were not known during the grafting procedure.) In previous studies, similar ventral diencephalon tissue preparations have been used for time-lapse video microscopy analysis of RGC axon growth (Sretavan and Reichardt, 1993; Godement et al., 1994), and robust RGC axon growth is known to continue in similar preparations for up to 2–3 d (Sretavan et al., 1995).

Grafting experiments were performed in E12.5 embryos before the arrival of RGC axons at the chiasm–tract transition zone. After placement of DiI-labeled retinal tissues onto the host ventral diencephalon, preparations were cultured, and the pattern and extent of axon outgrowth from grafted retinal tissue was examined after 40 hr. The pattern of RGC axon outgrowth from wild-type retinal grafts on wild-type diencephalon hosts mimicked that of RGC axons growing *in vivo* from the ventral midline into the initial portion of the optic tract (Fig. 6*B*,*C*). Although occasionally some graft axons grow back along the optic nerve and some axons project posteriorly into the ventral diencephalon, overall, the pattern of outgrowth primarily remained confined to the pathways taken by endogenous RGC axons *in vivo*. Most importantly RGC axons extended laterally >500 μm (Fig. 6*C*, *dotted line*) beyond the midline into the optic tract region. Furthermore, the width of the "pathway" containing graft axons (Fig. 6*C*, *distance* between *arrows*) approximately corresponded to the width of the pathway *in vivo* consisting of the main RGC axon bundle together with the region occupied by the more posteriorly located RGC axons (see Fig. 3*A*). Thus graft retinal axons seem to recognize guidance cues involved in RGC axon growth within the ventral diencephalon and through the transition zone into the optic tract.

In control experiments, labeled axons were observed only after grafting of living retinal tissue onto the host diencephalon. Identical retinal grafts labeled in the same manner but that have been pre-fixed with 4% paraformaldehyde did not elaborate retinal axons, and no labeled axons were seen in the host diencephalon. Likewise, DiI-labeled living liver tissue grafts, similar in size and shape to retinal grafts, when placed onto diencephalon host preparations and cultured for 40 hr, did not result in any labeled axons in host tissues (Fig. 6*D*,*E*). These experiments confirmed that labeled axons originated from the retinal grafts and not axons in the host tissue.

At the transition zone, axons from retinal grafts, like RGC axons *in vivo* at this age, extended within the diencephalon confined to a superficial region near the pial surface (Fig. 6*F*,*G*).

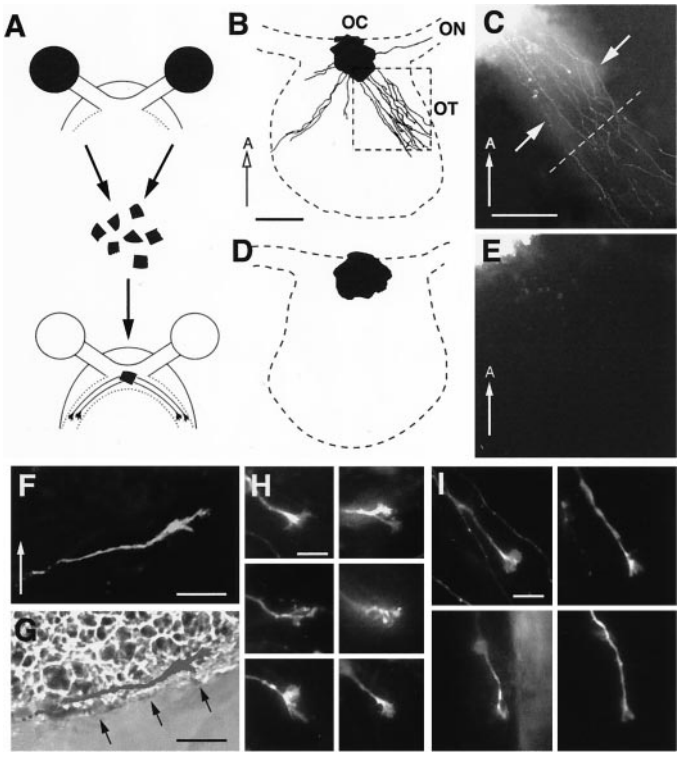

Figure 6. Axon outgrowth from retinal grafts into host diencephalon tissue preparations. *A*, Schematic diagram illustrating the experimental paradigm used in mix-and-match retinal grafting experiments. Retinal tissue (*black*) from a donor embryo (*top*) is harvested, labeled with DiI, and place at the ventral midline of a host embryo (*bottom*). Experiments were performed in E12.5 embryos, an age when optic tracts have yet to form. *B*, Schematic line drawing of a wild-type host ventral diencephalon preparation 40 hr after the grafting of DiI-labeled wild-type retinal tissue at the ventral midline. The *solid lines* represent DiI-labeled axons growing from the retinal graft (*black*) into the host. Note that axons do not grow randomly on the host tissue but instead preferentially extend along regions of the optic nerve (*ON*), chiasm (*OC*), and optic tracts (*OT*). The area *outlined* by the *rectangular box* is shown in *C*. Scale bar, 200 μm. *C*, Photograph showing DiI-labeled RGC axons illustrated in the *rectangular box* in *B*. The *dotted line* represents a distance 500 μm away from the ventral midline. Scale bar, 200 μm. *D*, Schematic line drawing of a E13 wild-type host ventral diencephalon preparation 40 hr after the grafting of DiI-labeled adult liver tissue at the ventral midline. No DiI-labeled axons are seen within the host tissue. Scale bar, 200 μm. *E*, Photograph of the host diencephalon preparation in *D* showing a portion of the DiI-labeled liver graft (*upper left corner*) and the lack of DiI-labeled axons in the host tissue. Scale bar, 200 μm. *F*, Photograph of a DiI-labeled RGC axon and growth cone extending from a retinal graft into a host diencephalon preparation. Scale bar, 10 μm. *G*, Double-exposure photograph (of *F*) showing the cells within the host diencephalon and the DiI-labeled axon and growth cone. Axons from retinal grafts grow within the host tissue just below the pial surface (*arrows*), mirroring the behavior of RGC axons *in vivo*. Scale bar, 10 μm. *H*, Six examples of growth cones from retinal grafts within the optic chiasm region of host diencephalon preparations. These growth cones, like growth cones at the chiasm *in vivo*, have a relatively more complex morphology than do growth cones in the optic tract region (see *I*). Scale bar, 10 μm. *I*, Four examples of growth cones from retinal grafts within the optic tract region of host diencephalon preparations. Within the optic tract, growth cones from retinal grafts, like growth cones *in vivo*, have a simple growth cone morphology. Scale bar, 10 μm.

Furthermore, the growth cones of graft axons in both the optic chiasm region (Fig. 6*H*) and the optic tract region (Fig. 6*I*) exhibited growth cones that morphologically closely resembled those found on RGC axons at these two sites *in vivo* (Bovolenta and Mason, 1987; Sretavan and Reichardt, 1993; Godement et al., 1994; Mason and Wang, 1997). Together, the overall pattern of axon outgrowth along the endogenous pathways, the growth of graft axons superficially in diencephalic tissue, and similarities in growth cone morphology indicated that graft RGC axons extending in the host diencephalon appear to respond to many of the same guidance cues governing RGC axon guidance *in vivo*.

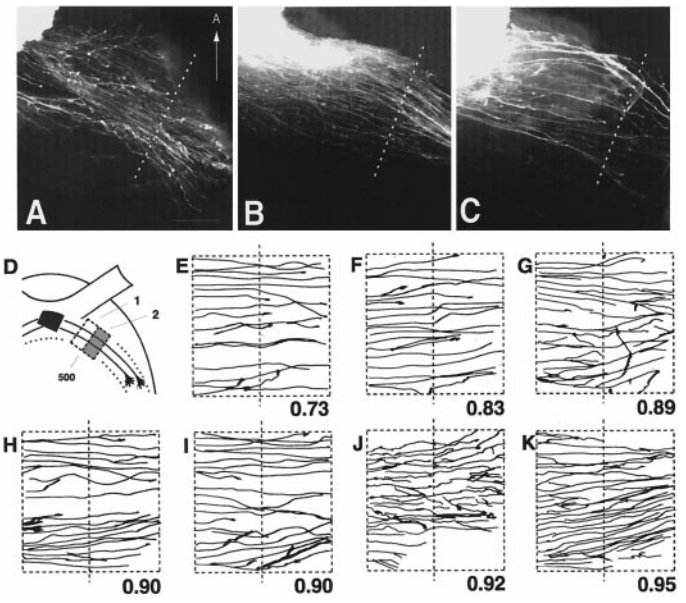

Figure 7. *A–C*, Axon outgrowth patterns from wild-type retinas grafted onto wild-type (*A*), heterozygous (*B*), or homozygous null (*C*) host diencephalon preparations. The *dotted line* in each *panel* indicates a position 500 μm away from the midline and is drawn approximately perpendicular to the general course of the labeled graft axons. The ventral midline is toward the *left* but is not included. Scale bar, 100 μm. *D*, Schematic diagram outlining the regions selected for quantitative measure of the degree of graft axon growth into the lateral wall of the diencephalon. The *rectangular boxes* represent the *regions* 100 × 200 μm in size that are located at a distance 400–500 μm away from the midline (*region 1*) and 500–600 μm away from the midline (*region 2*). The amount of graft axon in *region 2* is expressed as a fraction of the amount of axon in *region 1* and is referred to as the growth index. *E*, *F*, Pattern of axon growth after grafting wild-type retinal tissue onto wild-type host diencephalon. Only graft axons in *regions* 1 and 2 are represented. The *dotted line* in the center is 500 μm from the midline. The *number* below each *panel* represents the growth index. *G*, *H*, Pattern of axon growth after grafting wild-type retinal tissue onto heterozygote host diencephalon. *I–K*, Pattern of axon growth after grafting wild-type retinal tissue onto GAP-43 homozygous null host diencephalon.

Cell autonomous GAP-43 function in RGC axons

The mix-and-match grafting experiments resulted in nine different combinations of wild-type, heterozygous, or homozygous retinal tissue grafted onto host diencephalon of all three genotypes. Wild-type retinal grafts when placed onto host diencephalons of either wild-type ($n = 8$) (Fig. 7*A*,*E*,*F*), heterozygous ($n = 11$) (Fig. 7*B*,*G*,*H*), or homozygous null ($n = 6$) (Fig. 7*C*,*I–K*) genotypes all exhibited a similar pattern of outgrowth in which axons extended laterally in fairly straight trajectories for distances >500 μm from the midline (Fig. 7*A–C*,*E–K*, *dotted lines*) into the initial portion of the optic tract. To provide a quantitative measure of the degree of growth into the lateral wall of the diencephalon, the amount of graft axon growth between 500 and 600 μm from the midline was quantified and expressed as a fraction of axon growth in the region 400–500 μm from the

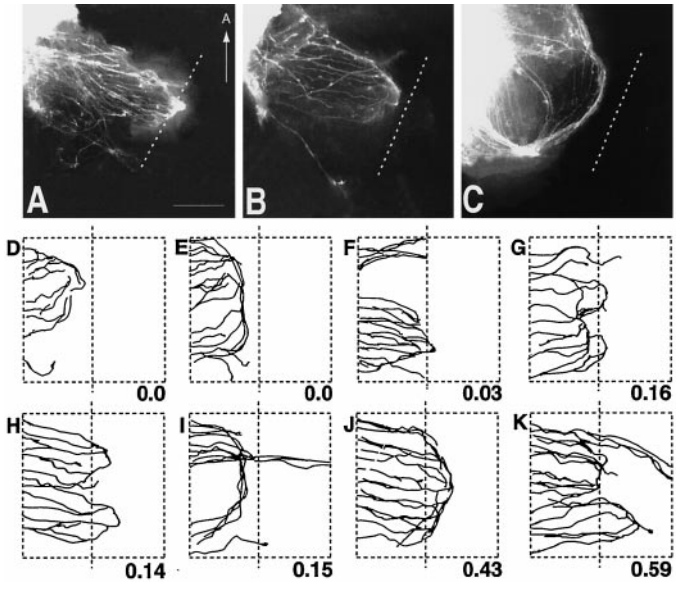

Figure 8. *A–C*, Axon outgrowth patterns from homozygous GAP-43 null retinas grafted onto wild-type (*A*), heterozygous (*B*), or homozygous null (*C*) host diencephalon preparations. The *dotted line* in each *panel* indicates a position 500 μm away from the midline. The ventral midline is toward the *left* but not included. Scale bar, 100 μm. *D–F*, Pattern of axon growth after grafting homozygous GAP-43 null retinal tissue onto wild-type host diencephalon. Only graft axons in *regions* 1 and 2 are represented. The *dotted line* in the center is 500 μm from the midline. The *number* below each *panel* represents the growth index. *G*, *H*, Pattern of axon growth after grafting homozygous GAP-43 null retinal tissue onto heterozygote host diencephalon. *I–K*, Pattern of axon growth after grafting homozygous GAP-43 null retinal tissue onto homozygous GAP-43 null host diencephalon. Note that occasionally a few graft axons do extend beyond 500 μm from the midline (*I*, *K*). However the bulk of axons still appear to stop near this site.

midline (referred to as the growth index). Graft experiments that resulted in RGC axons growing without apparent difficulty through the transition zone 500 μm from the midline would have growth indices approaching 1 (Fig. 7, range, 0.73–0.95). The turning away of graft axons at the transition zone would be expected to result in lower growth indices (see Fig. 8).

Experiments in which retinal tissue from heterozygous embryos was grafted onto either wild-type, heterozygous, or homozygous host tissues gave results identical to that in experiments with grafts using wild-type retinal tissues. Thus wild-type and heterozygous retinal axons appeared to have no difficulty in progressing from the chiasm through the transition zone to enter the lateral diencephalic wall where the optic tract is normally formed. Furthermore, the genotype of the diencephalic tissue seemed to have no influence on this behavior.

In contrast, homozygous null retinal tissue when grafted onto wild-type ($n = 6$) (Fig. 8*A*,*D–F*), heterozygous ($n = 13$) (Fig. 8*B*,*G*,*H*), or homozygous null ($n = 4$) (Fig. 8*C*,*I–K*) host preparations elaborated a quite different pattern of axonal growth. Although GAP-43 null retinal grafts extended axons, these axons in general did not progress beyond 500 μm away from the midline (Fig. 8, *dotted lines*) and appeared to stop short of entering the initial portion of the optic tract. Instead graft axons formed a foreshortened projection in which some axons appeared to turn away from the entrance of the optic tract (growth indices, 0–0.61), reminiscent of the axon trajectories observed in homozygous null embryos *in vivo* (compare Figs. 8 with 4*D*). Note however that occasionally a few graft axons do extend beyond 500 μm from the midline (Fig. 8*I*,*K*), although the majority of graft axon growth is clearly different to that seen after the grafting of wild-type or heterozygote retinal tissues (Fig. 7). The genotype of the diencephalon host tissue did not seem to influence greatly the pattern and extent of graft axon outgrowth, although variation was sometimes observed (compare Fig. 8*A*,*B* with *C*). These results indicated that the *in vivo* failure of RGC axons to progress from the chiasm into the diencephalic wall to form the optic tract was mimicked only when GAP-43 homozygous null retinal tissue was used as the graft. This observation is consistent with a pathfinding mechanism at the transition zone in which successful RGC axon passage requires cell autonomous GAP-43 function in RGC axons.

DISCUSSION

Results from this study demonstrate that an RGC axon pathfinding event critically dependent on GAP-43 function takes place at the transition zone between the optic chiasm and the optic tract. At this site, RGC axons in GAP-43 homozygous null embryos turn away from the lateral diencephalic wall to grow back within the chiasm and fail to form the optic tract. Although RGC axon passage through the chiasm–tract transition zone is affected in the absence of GAP-43, other axon populations, such as axons of CD44/SSEA neurons that also express GAP-43, are not perturbed in their ability to grow dorsally within the diencephalic wall in homozygous null embryos. This observation raises the possibility that different axon populations interact with distinct guidance cues in the transition zone, only some of which involve GAP-43 in their signaling cascade. Alternatively, because CD44/SSEA axons precede RGC axons through the transition zone, it may be that guidance mechanisms requiring GAP-43 function appear only after a precise developmental time. Results from experiments in which retinal tissue from wild-type, heterozygous, or homozygous null embryos was grafted onto diencephalon preparations from hosts of all three genotypes were consistent with a requirement for GAP-43 acting cell autonomously within RGC axons and not in other GAP-43–expressing cellular elements present in the transition zone.

Together, these results show that RGC axon progression from the chiasm into the optic tract involves a previously not generally recognized pathfinding event. Furthermore, development of the retinal pathway involves both GAP-43–dependent and –independent axon guidance mechanisms. GAP-43–independent guidance appears to occur in the first half of the pathway and includes pathfinding events such as RGC axon growth toward the optic disk, exit through the optic disk, entry into the ventral diencephalon, and crossing the ventral midline. The first apparent GAP-43–dependent guidance mechanism is involved in RGC axon progression from the optic chiasm into the lateral diencephalic wall to initiate the optic tract.

Changes at the transition zone

The presence of a pathfinding defect at the optic chiasm–optic tract transition zone indicates that RGC axons normally encounter a change in their growth environment at this site. Two characteristics of RGC axon growth within the chiasm compared with growth within the tract are consistent with this possibility. First, RGC axons in mice are known to enter the chiasm in a dispersed manner as they sort out from each other to project into the ipsilateral and contralateral optic tracts (Colello and Guillery, 1990; Godement et al., 1990; Sretavan, 1990). As RGC axons

grow further lateral away from the ventral midline, they again become more tightly bundled (perhaps fasiculated) with each other as they pass into the optic tract (Reese et al., 1994) (Figs. 3*A*, 4*A*). Second, ultrastructural studies have demonstrated that embryonic RGC axons in the chiasm grow deep within the diencephalic tissue, only to surface into a more superficial position underneath the pia after they enter the tract (Colello and Coleman, 1997). Both observations suggest that guidance mechanisms at the chiasm and in the initial portions of the optic tract are sufficiently distinct to result in different RGC axon growth characteristics in these two adjoining segments of the visual pathway.

The basis of such differences is not known. In the adult visual system of the ferret, axon–glia interactions involved in myelination apparently differ in the optic nerve and the optic tract and are reflected in a change in the conduction velocity of RGC axons measured at these two sites (Baker and Stryker, 1990). It is not known where precisely between the optic nerve and the optic tract this change in axon interaction with its glial environment takes place. Nevertheless, the finding that axon–glia interactions do differ in various segments of the adult retinal pathway raises the possibility that during embryonic development, RGC axon progression from the chiasm into the optic tract might involve changes in axon–glia interaction at these adjoining sites. Indeed, differences in the density of vimentin-positive glial processes have been noted between the optic chiasm and the diencephalon deep to the optic tract in embryonic ferrets (Reese et al., 1994).

Which guidance molecules are involved?

The data from this study are consistent with a model in which a guidance mechanism requiring GAP-43 function in RGC axons is involved in axon passage through the transition zone. The nature of the molecular cues involved are as yet unknown, but in principle interaction with these guidance cues could either act to promote the growth of RGC axons into the lateral diencephalic wall or act to inhibit RGC axon growth resulting in fasiculated axon growth confined to a tightly bundled pathway in the diencephalic wall. In this latter case, GAP-43 function may be required to dampen RGC axon response to inhibition, allowing axon elongation. In the absence of GAP-43 function, unmodulated inhibition prevents RGC axon growth. Of note, studies in which GAP-43 function in dorsal root ganglion axons was perturbed using antisense oligonucleotides showed that treated growth cones were more prone to collapse compared with untreated axons when confronted with CNS myelin protein-containing liposomes (Aigner and Caroni, 1995).

The finding that RGC axon growth out of the retina, into the ventral diencephalon, and across the midline was not affected in GAP-43 homozygous null embryos may help eliminate certain guidance cues as candidates involved in GAP-43–dependent axon guidance at the transition zone. Because RGC axon growth within the retina and exit from the eye do not seem to be affected, this suggests that GAP-43 is not involved in guidance mediated by cadherins, which underlie axon outgrowth from RGCs (Riehl et al., 1996), and DCC, which via interaction with netrin-1 governs RGC axon exit at the disk into the nerve (Deiner et al., 1997).

Along this same line of reasoning, given that RGC axon guidance before the transition zone appears normal, the relevant guidance cues might not be present earlier in the retinal pathway before the transition zone. This supposition is however subject to caution, because it is not possible to completely eliminate redundant RGC axon guidance mechanisms existing in other parts of the pathway that are capable of substituting for the lack of GAP-43, but such redundancy is not present at the transition zone, and a pathfinding defect manifests at this site in GAP-43 null embryos. Furthermore, it is also possible that RGC axons only begin to express the receptor for a particular guidance cue as they exit from the chiasm, and thus although the same guidance cue may be present in other parts of the retinal pathway, RGC axons lacking GAP-43 may not be affected until reaching the transition zone.

In a previous study, the application of protein kinase inhibitors herbimycin A and lavendustin A to exposed brain preparations in frog embryos resulted in the failure of RGC axons to grow into the lateral wall of the diencephalon (Worley et al., 1997), a phenotype resembling that described here for GAP-43 homozygous null mouse embryos. This finding in the frog visual system suggests that kinase activity is important for RGC axon growth in the diencephalon. However, because inhibitors were added at a developmental time when RGC axons were just beginning to grow into the optic tract, it is likely that kinase activity is generally involved in axon elongation and not necessarily specific to RGC axon ingrowth into the lateral diencephalic wall. However, given the involvement of Eph receptor kinases and their ligands in RGC axon mapping in visual targets (Nakamoto et al., 1996; Frisen et al., 1998), it is possible that guidance cues that alter phosphorylation states in RGC axons might be involved in axon passage through the chiasm–tract transition zone.

Differential effects on RGC axons versus CD44/SSEA axons

Results from this study show that RGC axons are not the only axon population that express GAP-43 and grow from the ventral diencephalon into the lateral diencephalic wall. In fact, axons belonging to CD44/SSEA neurons, an early generated cell population positioned at the posterior border of the future optic chiasm, precede RGC axons into the lateral diencephalon by 2 d. Although both axonal populations grow into the lateral diencephalic wall, the axons of CD44/SSEA neurons were not affected while RGC axons failed to enter to initiate development of the optic tract. One explanation for this differential effect on these two axon populations is that they travel in adjacent but nonoverlapping paths to enter the diencephalic wall and thus may encounter different guidance cues. Guidance cues in one path trigger GAP-43–dependent guidance, whereas others in the second path do not. This explanation is however not supported by the anatomical evidence that demonstrate that at least some RGC axons are intermixed with axons of CD44/SSEA neurons, and thus both axon populations spatially grow through the same region (Fig. 5*B*,*C*). Given this finding, a modified explanation is that RGC axons and CD44/SSEA axons growing through the same region do not respond to the same guidance cues and that GAP-43–dependent axon guidance in the lateral diencephalic wall is RGC axon-specific.

A second explanation that should be considered is that although both axon populations grow through the same region spatially, they do not do so at the same developmental time. It is therefore possible that the guidance cue environment of the transition zone itself changes in the 2 d interval between CD44/SSEA axon and RGC axon passage through this region. One line of evidence supporting the possibility of changes occurring in the transition zone environment is the fact that RGC axons in GAP-43 homozygous null embryos do eventually enter the diencephalic wall to establish the optic tract (Strittmatter et al., 1995).

We have found that the delayed optic tracts that are first detected as early as E17–E18 originate from the very same RGC axons that initially could not grow into the lateral diencephalic wall and instead grew in abnormal trajectories within the chiasm (K. Kruger and D. Sretavan, unpublished observations). The subsequent ability of these GAP-43 null RGC axons with abnormal trajectories to grow into the lateral diencephalic wall a few days later can best be explained by a change in the cellular and molecular environment of the transition zone. If this proves correct, taken together, the ability of CD44/SSEA axons to enter at E11 but not RGC axons to enter at E13–E14 and the eventual entry of RGC axons into the lateral diencephalic wall at E17–E18 suggest that dynamic changes in the molecular environment of the transition zone occur during formation of the optic tract and that a time window between E11–E13 and E17–E18 exists in which the transition zone triggers GAP-43–dependent axon guidance in RGC axons.

Multiple RGC pathfinding tasks during optic chiasm development

Previous studies investigating how RGC axons establish the optic chiasm during embryonic development have identified a number of pathfinding tasks that RGC axons perform after entry into the ventral diencephalon from the optic nerve. These include the positioning of the optic chiasm on the surface of the ventral diencephalon (Sretavan et al., 1994, 1995), the specific sorting of axons into the ipsilateral and contralateral optic tracts (for review, see Mason and Sretavan, 1997), and rearrangement of RGC axon topographic order within the chiasm (Reese and Baker, 1990; Reese et al., 1994). The results from this paper add to this list the task of properly exiting out of the optic chiasm to form the optic tract. Almost certainly, the ability of RGC axons to accomplish all of these developmental tasks requires well-orchestrated interactions with specific cues that may be highly localized to certain subregions of the ventral diencephalon or on subpopulations of RGC axons. In one sense this makes *in vitro* assays of RGC axon pathfinding more difficult, but the identification of these separate pathfinding tasks should also allow us to design more specific experiments.

A problem of exit or entry?

Although the present data indicate that GAP-43 function is required in RGC axons for successful passage through the chiasm–tract transition zone, they do not specify whether GAP-43 is involved in the ability of RGC axons to exit from the chiasm after they have accomplished a number of pathfinding tasks or whether it is needed for RGC axons to enter a new territory, the lateral diencephalic wall. For instance, the chiasm region clearly provides an environment conducive for RGC axon interaction with multiple guidance mechanisms. It seems likely that to leave this environment, RGC axons might be required to undergo changes in guidance receptor expression or alterations in signaling pathways, events that may involve calmodulin or G-protein function mediated by GAP-43. In the same vein, the entry into the lateral diencephalic wall might involve GAP-43, the proper function of which may be required for RGC axons to respond appropriately to a new set of guidance cues that they may encounter on entering the lateral diencephalic wall. The answer to this question of exit versus entry will dictate to a large extent the design of experiments exploring in greater detail how GAP-43 functions in RGC axon pathfinding.

REFERENCES

Aigner L, Caroni P (1993) Depletion of 43 kDa growth-associated protein in primary sensory neurons leads to diminished formation and spreading of growth cones. J Cell Biol 123:417–429.

Aigner L, Caroni P (1995) Absence of persistent spreading, branching, and adhesion in GAP-43-depleted growth cones. J Cell Biol 128:647–660.

Aigner L, Arber S, Kapfhammer JP, Laux T, Schneider C, Botteri F, Brenner HR, Caroni P (1995) Overexpression of the neural growth-associated protein GAP-43 induces nerve sprouting in the adult nervous system of transgenic mice. Cell 83:269–278.

Alexander KA, Wakim BT, Doyle GS, Walsh KA, Storm DR (1988) Identification and characterization of the calmodulin-binding domain of neuromodulin, a neurospecific calmodulin-binding protein. J Biol Chem 263:7544–7549.

Baker GE, Stryker MP (1990) Retinofugal fibres change conduction velocity and diameter between the optic nerve and tract in ferrets. Nature 344:342–345.

Benowitz LI, Routtenberg A (1997) GAP-43: an intrinsic determinant of neuronal development and plasticity. Trends Neurosci 20:84–91.

Bovolenta P, Mason C (1987) Growth cone morphology varies with position in the developing mouse visual pathway from retina to first targets. J Neurosci 7:1447–1460.

Brittis PA, Silver J (1995) Multiple factors govern intraretinal axon guidance: a time-lapse study. Mol Cell Neurosci 6:413–432.

Brittis PA, Canning DR, Silver J (1992) Chondroitin sulfate as a regulator of neuronal patterning in the retina. Science 255:733–736.

Chan SO, Guillery RW (1994) Changes in fiber order in the optic nerve and tract of rat embryos. J Comp Neurol 344:20–32.

Colello SJ, Coleman L (1997) Changing course of growing axons in the optic chiasm of the mouse. J Comp Neurol 379:495–514.

Colello RJ, Guillery RW (1990) The early development of retinal ganglion cells with uncrossed axons in the mouse: retinal position and axon course. Development 108:515–523.

Curtis R, Stewart HJS, Hall SM, Wilkin GP, Mirsky R, Jessen KR (1992) GAP-43 is expressed by nonmyelin-forming Schwann cells of the peripheral nervous system. J Cell Biol 116:1455–1464.

Deiner MS, Kennedy T, Fazeli A, Serafini T, Tessier-Lavigne M, Sretavan DW (1997) Netrin-1 and DCC mediate axon guidance locally at the optic disc: loss of function leads to optic nerve hypoplasia. Neuron 19:575–589.

Deloulme J-C, Janet T, Au D, Storm DR, Sensenbrenner M, Baudier J (1990) Neuromodulin (GAP43): a neuronal protein kinase C substrate is also present in 0–2A glial cell lineage. Characterization of neuromodulin in secondary cultures of oligodendrocytes and comparison with the neuronal antigen. J Cell Biol 111:1559–1569.

Easter SS, Ross LS, Frankfurter A (1993) Initial tract formation in the mouse brain. J Neurosci 13:285–299.

Frisen J, Yates PA, McLaughlin T, Friedman G, O'Leary DDM, Barbacid M (1998) Ephrin-A5 (AL-1/RAGS) is essential for proper retinal axon guidance and topographic mapping in the mammalian visual system. Neuron 20:235–243.

Godement P, Salaun J, Mason CA (1990) Retinal axon pathfinding in the optic chiasm: divergence of crossed and uncrossed fibers. Neuron 5:173–186.

Godement P, Wang LC, Mason CA (1994) Retinal axon divergence in the optic chiasm: dynamics of growth cone behavior at the midline. J Neurosci 14:7024–7039.

Jacobson RD, Virag I, Skene JHP (1986) A protein associated with axon growth, GAP-43, is widely distributed and developmentally regulated in rat CNS. J Neurosci 6:1843–1855.

Lilienbaum A, Reszka AA, Horwitz AF, Holt CE (1995) Chimeric integrins expressed in retinal ganglion cells impair process outgrowth in vivo. Mol Cell Neurosci 6:139–152.

Marcus R, Mason C (1995) The first retinal axon growth in the mouse optic chiasm, axon patterning and the cellular environment. J Neurosci 15:6389–6402.

Mason CA, Sretavan DW (1997) Glia, neurons, and axon pathfinding during optic chiasm development. Curr Opin Neurobiol 7:647–653.

Mason CA, Wang LC (1997) Growth cone form is behavior-specific and, consequently, position-specific along the retinal axon pathway. J Neurosci 17:1086–1100.

McFarlane S, McNeill L, Holt CE (1995) FGF signaling and target recognition in the developing *Xenopus* visual system. Neuron 15:1017–1028.

Nakamoto M, Cheng H-J, Friedman GC, McLaughlin T, Hansen MJ, Yoon CH, O'Leary DDM, Flanagan JG (1996) Topographically specific effects of ELF-1 on retinal axon guidance in vitro and retinal axon mapping in vivo. Cell 86:755–766.

Orioli D, Klein R (1997) The Eph receptor family: axonal guidance by contact repulsion. Trends Genet 13:354–359.

Reese B, Cowey A (1988) Segregation of functionally distinct axons in the monkey's optic tract. Nature 331:350–351.

Reese BE, Baker GE (1990) The course of fibre diameter classes through the chiasmatic region in the ferret. Eur J Neurosci 2:34–49.

Reese BE, Maynard TM, Hocking DR (1994) Glial domains and axonal reordering in the chiasmatic region of the developing ferret. J Comp Neurol 349:303–324.

Riehl R, Johnson K, Bradley R, Grunwald GB, Cornel E, Lilienbaum A, Holt CE (1996) Cadherin function is required for axon outgrowth in retinal ganglion cells in vivo. Neuron 17:837–848.

Shea TB (1994) Delivery of anti-GAP-43 antibodies into neuroblastoma cells reduces growth cone size. Biochem Biophys Res Commun 203:459–464.

Shea TB, Benowitz LI (1995) Inhibition of neurite outgrowth following intracellular delivery of anti-GAP-43 antibodies depends upon culture conditions and method of neurite induction. J Neurosci Res 41:347–354.

Skene JHP (1990) GAP-43 as a "calmodulin sponge" and some implications for calcium signalling in axon terminals. Neurosci Res 13:S112–S125.

Skene JHP, Virag I (1989) Posttranslational membrane attachment and dynamic fatty acylation of a neuronal growth cone protein, GAP-43. J Cell Biol 108:613–624.

Sretavan DW (1990) Specific routing of retinal ganglion cell axons at the mammalian optic chiasm during embryonic development. J Neurosci 10:1995–2007.

Sretavan DW (1993) Pathfinding at the mammalian optic chiasm. Curr Opin Neurobiol 3:45–52.

Sretavan DW, Reichardt LF (1993) Time-lapse video analysis of retinal ganglion cell axon pathfinding at the mammalian optic chiasm: growth cone guidance using intrinsic chiasm cues. Neuron 10:761–777.

Sretavan DW, Feng L, Pure E, Reichardt LF (1994) Embryonic neurons of the developing optic chiasm express L1 and CD44 cell surface molecules with opposing effects on retinal axon growth. Neuron 12:957–975.

Sretavan DW, Pure E, Siegel MW, Reichardt LF (1995) Disruption of retinal axon ingrowth by ablation of embryonic mouse optic chiasm neurons. Science 269:98–101.

Strittmatter SM, Valenzuela D, Kennedy TE, Neer EJ, Fishman MC (1990) G_o is a major growth cone protein subject to regulation by GAP-43. Nature 344:836–841.

Strittmatter SM, Fankhauser C, Huang PL, Mashimo H, Fishman MC (1995) Neuronal pathfinding is abnormal in mice lacking the neuronal growth cone protein GAP-43. Cell 80:445–452.

Walz A, McFarlane S, Brickman YG, Nurcombe V, Bartlett PF, Holt CE (1997) Essential role of heparan sulfates in axon navigation and targeting in the developing visual system. Development 124:2421–2430.

Wang L-C, Dani J, Godement P, Marcus R, Mason CA (1995) Crossed and uncrossed retinal axons respond differently to cells of the optic chiasm midline in vitro. Neuron 15:1349–1364.

Worley TL, Cornel E, Holt CE (1997) Overexpression of c-src and n-src in the developing *Xenopus* retina differentially impairs axonogenesis. Mol Cell Neurosci 9:276–292.